10
SOLUTION MINING RESEARCH INSTITUTE

679 Plank Road
Clifton Park, NY 12065, USA

Telephone: +1 518-579-6587
www.solutionmining.org

Technical Conference Paper

1965 – 2025

The Bekendam-Jakob-Pinkse (BJP) subsidence prognosis algorithm for migrating salt caverns in a bedded salt deposit near Hengelo, The Netherlands

Christian Jakob

K-UTEC AG Salt Technologies, Sondershausen, Germany

Tobias Pinkse

REinvent Solutions B.V., The Hague, Netherlands

(formerly REinvent GmbH, Sondershausen, Germany)

Marinus den Hartogh

Els Wijermars

Paul Oonk

Siebe Viersen

Nobian Industrial Chemicals B.V., Hengelo, The Netherlands

SMRI Spring 2025 Technical Conference
27-29 April 2025
Wilhelmshaven, Germany

Solution Mining Research Institute Spring 2025 Conference

Wilhelmshaven, Germany, 27-29 April 2025

The Bekendam-Jakob-Pinkse (BJP) subsidence prognosis algorithm for migrating salt caverns in a bedded salt deposit near Hengelo, The Netherlands

Dr.-Ing. Christian Jakob*, Tobias Pinkse M.Sc.**, Marinus den Hartogh M.Sc.***,

Els Wijermars M.Sc.***, Dr. Paul Oonk***, Siebe Viersen M.Sc.***

* K-UTEC AG Salt Technologies, Sondershausen, Germany
** REinvent Solutions B.V., The Hague, Netherlands
(formerly REinvent GmbH, Sondershausen, Germany)
*** Nobian Industrial Chemicals B.V., Hengelo, The Netherlands

Abstract

The historic development of the Nobian cavern field in the Twenthe-Rijn (TWR) mining permit (incl. extensions) has been divided into five phases based on the cavern development strategy and technological developments since the nineteen thirties. (The late) Roland Bekendam prepared a cavern migration model for caverns developed during “Phase 1” and “Phase 2” as presented during the 1997 SMRI Spring meeting in Krakow (Bekendam, 1997). Development of caverns in this area commenced from the 1930’s up to the 1970’s. During this period, measures to control the leaching process such as the use of a blanket medium and regular sonar surveys were not available or in the early stages of development and application. Roof stability of a number of caverns was severely compromised and led to upward migration of caverns. The Bekendam method enabled preparation of subsidence prognoses over migrating caverns and allowed Nobian to devise a backfilling strategy using brine purification residues as a resource. The prepared prognoses allowed for a prioritisation of backfilling efforts for caverns which could potentially lead to sinkholes. Since 1975 Nobian has developed caverns for which roof instability is no longer a concern. Hence, this study is on early developed caverns.

New data, information and insights were gained since the initial development of the Bekendam method in the 1990’s which permitted an elaborate update of the method. The update was aimed at addressing several processes relevant to cavern migration which were not included historically. The new Bekendam-Jakob-Pinkse (BJP) algorithm is thus an analytical/empirical extension of the historically used Bekendam method. The BJP Algorithm has been validated using 10 well-documented cavern migration cases from the Hengelo cavern field. After its validation, the BJP Algorithm has been applied to a set of early developed caverns in the TWR area to establish the likelihood of potential migration and to determine the total subsidence if migration occurs.

In conclusion, the study showed that a large number of caverns can now be classified as stable and/or intrinsically safe. This means that these caverns cannot cause a significant effect at surface. This facilitates a significant reduction of the overall time and material volume needed to backfill relevant caverns in the Hengelo area. Completion of the required backfilling based on the outcome of the BJP Algorithm is deemed attainable within a “single generation” rather than taking well over a century, thereby reducing Nobian’s risk exposure.

Key words: salt caverns, cavern abandonment, rock mechanics, subsidence

Introduction

The historic development of the Nobian cavern field in the Twenthe-Rijn (TWR) mining permit (incl. extensions) has been divided into five phases based on the cavern development strategy and technological developments since the nineteen thirties, see Figure 1. Development of caverns in the phases 1 and 2 commenced from the 1930's up to the 1970's. During this period, measures to control the leaching process such as the use of a blanket medium and regular sonar surveys were not available or in the early stages of development and application. Roof stability of a number of caverns was severely compromised and led to upward migration of caverns. In some cases, the upward migration of caverns has led to substantial subsidence at surface. A sinkhole that developed around well TWR-070 in 1991, 14 years after production from this cavern was stopped, is the most prominent case of surface subsidence.

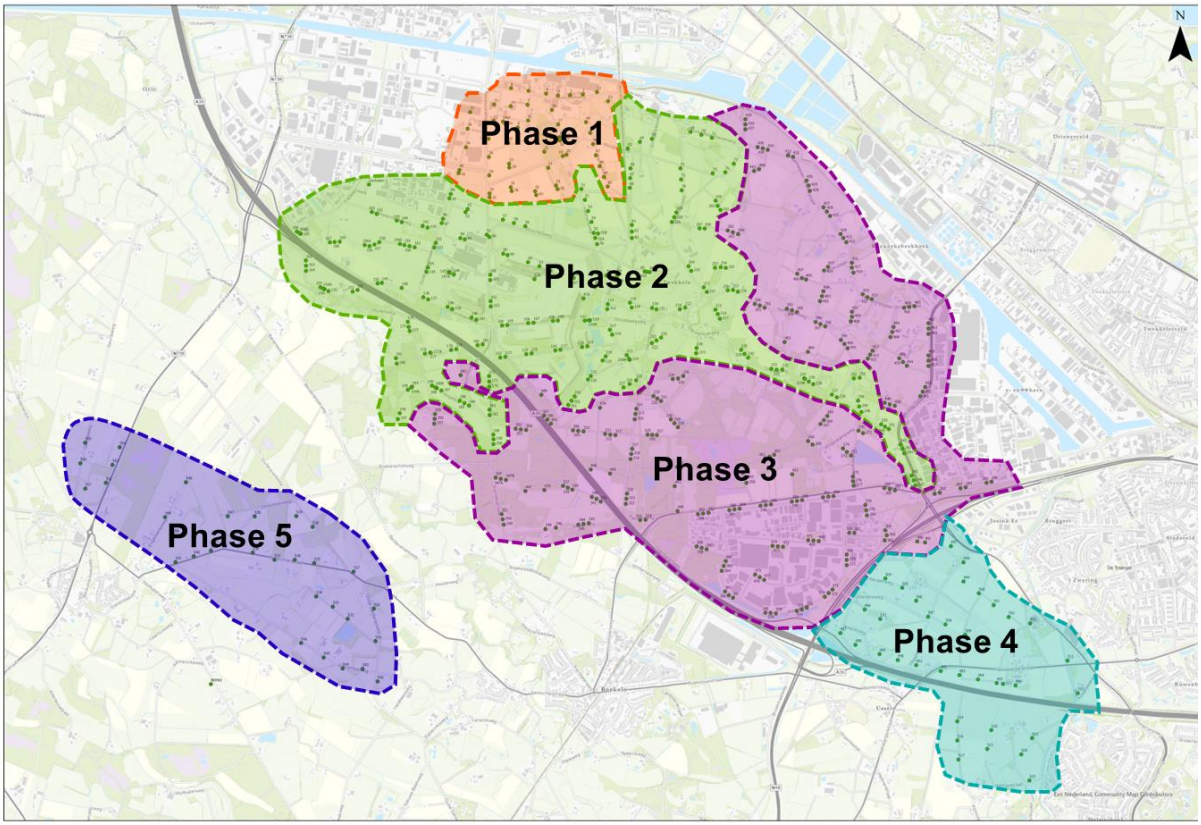

Figure 1. Historical development of TWR-area

After the occurrence of this sinkhole an extensive research project was started to evaluate if other (abandoned) caverns also carried this risk. The (late) Roland Bekendam prepared a cavern migration model referred to as the 'Bekendam method', for caverns developed during "Phase 1" and "Phase 2" as presented during the 1997 SMRI Spring meeting in Krakow (Bekendam, 1997). Although many aspects of the migration process were studied in great detail, the risk of cavern migration leading to severe subsidence was assessed based on two aspects:

- The chance of cavern migration depended on the composition and thickness of layers in the cavern roof. For caverns with a 'safety roof' that consists of an at least 5 m thick intact layer of salt across the entire roof span, migration was excluded. Caverns where this safety roof was not present were considered 'potentially instable' and were classified as caverns to be backfilled in the future, also if the safety roof was compromised only in a small part of the cavern and to a limited extent.
- The extent of the migration process was based on the cavern height and a bulking factor that was determined for the overburden. A cavern with a limited height will fill itself up during upwards migration due to the bulking effect of the layers collapsing into the cavern. Therefore, this process will stop deep in the subsurface and cause a limited amount of subsidence at surface. In this case a cavern is considered 'intrinsically safe'. A cavern with a relatively large height can migrate further upwards and when this process approaches the transition from rocks to unconsolidated

Tertiary sediments it can lead to severe subsidence such as a sinkhole. In this case a cavern is considered 'not intrinsically safe'. All caverns that had a height that was considered 'not intrinsically safe', were classified to be backfilled in the future, also if this height only occurred in a small part of the cavern.

These two aspects were very simple to assess for each cavern but also very conservative. This led to a list of 55 caverns which required backfilling. The backfill medium that is already applied since the start of the salt production of the Hengelo plant, is a residue of the brine purification process at the salt plant. The residue is produced as a suspension or slurry. It contains solid particles that settle on the cavern bottom and consequently reduce the cavern height. With sufficient backfill the cavern becomes intrinsically safe.

The volume of this brine purification residue is however limited and it takes several years to backfill a single cavern. Backfilling all 55 caverns to their maximum practically attainable filling grade with this material would take an unacceptable amount of time, passing this liability on to multiple future generations. Therefore, the possibility of applying alternative backfilling materials was investigated, which is beyond the scope of this paper. In addition, the necessity of backfilling caverns was re-evaluated. For this purpose, the cavern migration model was updated to a more realistic but still conservative model based on the latest data and knowledge.

New data, information and insights were gained since the initial development of the Bekendam method in the 1990's which permitted an elaborate update of the method. The update was aimed at addressing several processes relevant to cavern migration which were not included historically. The new Bekendam-Jakob-Pinkse (BJP) algorithm is thus an analytical/empirical extension of the historically used Bekendam method. The BJP Algorithm has been validated using well-documented cavern migration cases from the Hengelo cavern field. After its validation, the BJP Algorithm has been applied to a further 90+ caverns in the TWR area to establish the likelihood of potential migration and to determine the total subsidence if migration occurs.

After a brief geological introduction, the historically used Bekendam algorithm is discussed first to set a baseline for the recent study. The updated algorithm is explained next, followed by two examples of the cavern migration reconstruction performed to validate the updated algorithm. This paper finishes with conclusions and an outlook on future work anticipated as part of this ongoing study.

Geology of the TWR brinefield

In the Twenthe-Rijn Brinefield, salt was and is produced from the Triassic Main Röt evaporite. In the area, the Main Röt evaporite is around 70 m (230 ft) thick and lies between 300 to 520 mbgl (984 to 1706 ft). The Main Röt evaporite consists of four distinct halite beds [Salt A-D] interbedded with claystone and anhydrite layers (*labelled "claystone AB" for the bench between Salt A and Salt B etc.*). Overlying the Salt D (when present) is Anhydrite-E which consists of relative pure anhydrite and is 10-14 m (33-46 ft) thick. Other Röt formation members overly the Main Röt evaporite. The overburden consists mainly of claystones with distinct anhydrite beds (Table 1). The Muschelkalk thickness varies over a relatively small area due to erosional surfaces (GEOWULF Laboratories, 2008), resulting in varying thickness of the Jurassic formations. The unconsolidated Tertiary sands and clays of the North Sea Supergroup are generally around 100 m (328 ft) thick in the area. Their thickness plus an additional 40 m (131 ft) was used as the critical migration depth in the original Bekendam algorithm.

Geologic period	Group / Formation	Member	Dominant lithology	Thickness (m)	Thickness (ft)	Code
Tertiary	North Sea Supergroup		Unconsolidated sand / clay	60-150	197-492	N
Jurassic	Niedersachsen Group		Shale / claystone	0-65	0-213	SK
	Altena Group		Claystone	0-20	0-66	AT
Triassic	Muschelkalk Formation		Dolomite / claystone	20-120	66-394	RNMU
	Röt Formation	Upper Röt claystone	Claystone / anhydrite	120-150	394-492	RNROU- *[I-A]*
		Upper Röt evaporite	Anhydrite	1-3	3-10	RNRO2
		Interm. Röt claystone	Claystone / siltstone	30-40	98-131	RNROM- *[B-A]*

		Main Röt evaporite	Halite / anhydrite / claystone	30-100	98-328	RNRO1
	Solling Formation		Claystone / sandstone	80-100	262-328	RNSO

Table 1. Simplified geological overview of the Twenthe-Rijn Brinefield (GEOWULF Laboratories, 2008)

The Bekendam algorithm

The Bekendam subsidence prognosis algorithm was developed by (late) Roland F. Bekendam to estimate subsidence for migrating caverns in the Hengelo cavern field (Bekendam, 1997). By investigation of observed subsidence measurements, Bekendam distinguished three phases of subsidence:

- Phase I subsidence occurs due to creep deformation of the salt. Compared to subsidence of a migrated cavern the amount and rate of phase I subsidence is negligible.

- Phase II subsidence occurs, when the cavity migrates upward through the Top Anhydrite and the Claystone above. It was observed that cavities migrate at a rate of several feet/meters per year. In the Bekendam algorithm it was interpreted to result in a more or less constant subsidence rate of several mm per year, that would decrease to practically zero after the end of migration.

- Phase III subsidence occurs for caverns, which migrate near the base of Tertiary sediments. In these cases, a significant acceleration of subsidence followed by a continuously decreasing subsidence rate, was observed. The latter part of this type of subsidence will generally last for tens of years.

For the subsidence prognosis algorithm Bekendam used a critical depth of 40 m (131 ft) below the base of Tertiary sediments (top rock) to decide if a cavern can possibly lead to phase III subsidence. The migration height H_{mig} was calculated by a simple analytical approach for the bulking of the material during the migration process. The migration height only depends on the cavern height H_{cav} and the historically used bulking factor B.

$$H_{mig} = H_{cav}/(B-1)$$

Phase III subsidence was subdivided into three possible cases:

- “B only” occurs when the migration stops above the critical depth, but below top rock. In this case the deformation of the remaining roof layer of claystone will lead to a slow compaction of the bulked material in the migration column, which leads to subsidence called phase IIIB.

- “A + B” occurs when the migration reaches top rock with a remaining cavern height of less than 2 m (6.6 ft). This leads to a pronounced subsidence trough on surface, but not a sinkhole. In this case subsidence from the trough is called phase IIIA. In addition to phase IIIA, subsidence of phase IIIB will also occur over time in this case.

- A sinkhole occurs when the migration reaches top rock, but with a remaining cavern height of more than 2 m (6.6 ft). In addition to the subsidence from the sinkhole, phase IIIB subsidence will also occur over time in this case.

The radial expression of subsidence is calculated by the gaussian error function (erf) as follows.

$$\eta(r) = \frac{S}{2} \cdot erf\left(\frac{\sqrt{4\pi} \cdot r'}{R}\right) \cdot \left[erf\left(\frac{\sqrt{4\pi} \cdot (r'+r)}{R}\right) + erf\left(\frac{\sqrt{4\pi} \cdot (r'-r)}{R}\right)\right]$$

$$r' = \frac{\sqrt{\pi} \cdot R_{cav}}{2}$$

Here R is the radius of influence on surface, r' is the equivalent half-width of subsurface depression and S is the subsidence factor (representing the underground vertical movement, that effectively influences subsidence at the surface).

The calculation of phase II subsidence is an empirical analytical solution based on results of numerical simulations with different cavern radii (GeoControl, 2006).

$$S_{II} = \frac{(f_1 \cdot R_{cav}^3 + f_2 \cdot R_{cav}^2 + f_3 \cdot R_{cav}) \cdot \frac{H_{cav}}{20}}{\left[erf\left(\sqrt{4\pi} \cdot r'/R_{II}\right)\right]^2}$$

For calculation of the radius of influence for phase II the half height of the migration column d_{mig2} with an angle of draw of $\gamma = 45°$ is used (see Figure 1).

$$R_{II} = d_{mig2} \cdot \tan\gamma$$

For determination of phase III subsidence, the amount of phase IIIB is always added.

$$\eta_{III} = \eta_{IIIA} + \eta_{IIIB}$$

The amount of phase IIIB is calculated by consolidation (with coefficient C_{bulk}) of the bulked material (with a height of H_{bulk}) under the load of the Tertiary sediments (with mean weight γ_{sed} and thickness H_{sed}).

$$S_{IIIB} = \gamma_{sed} \cdot H_{sed} \cdot C_{bulk} \cdot H_{bulk}$$

The calculation of phase IIIA subsidence depends on the case. In the case “B only” it is zero. In the case of a trough, it is derived by using the remaining cavern height at top rock $H_{cav,TR}$ as subsidence factor.

$$S_{IIIA} = H_{cav,TR}$$

In the case of a sinkhole the subsidence within the range of the cavern radius is equal to the remaining cavern height at top rock.

$$\eta_{IIIA} = H_{cav,TR}$$

For determination of $H_{cav,TR}$ the bulking factor is used with the remaining migration distance between the critical depth d_{crit} and the depth, where migration process stops (denoted by d_{final}).

$$H_{cav,TR} = \left(d_{crit} - d_{final}\right) \cdot (B - 1)$$

Figure 2 illustrates the principle of the Bekendam algorithm for phase II and phase III. The total subsidence of phase II and III was derived by superposition of both subsidence amounts on a 2D coordinate grid with a resolution of 10 m (32,8 ft) in space. In doing so it is possible to plot prognoses of radial-symmetric subsidence troughs around caverns on a surface map (see Figure 3).

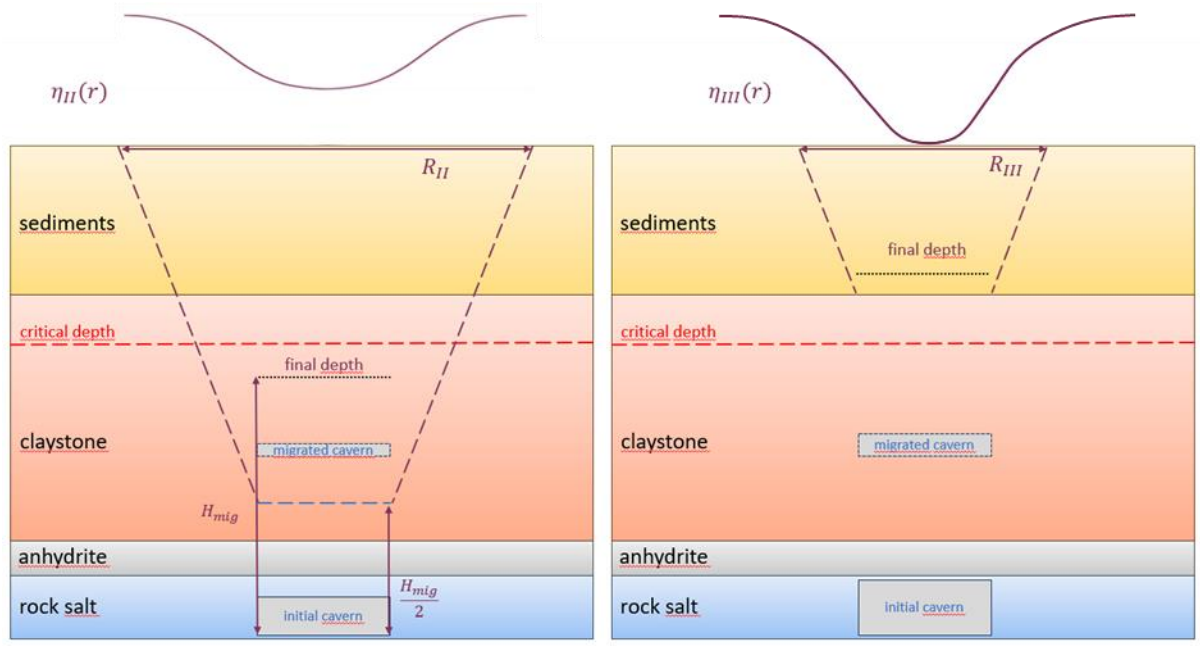

Figure 2. Schematic principle of phase II and phase III subsidence in the Bekendam algorithm

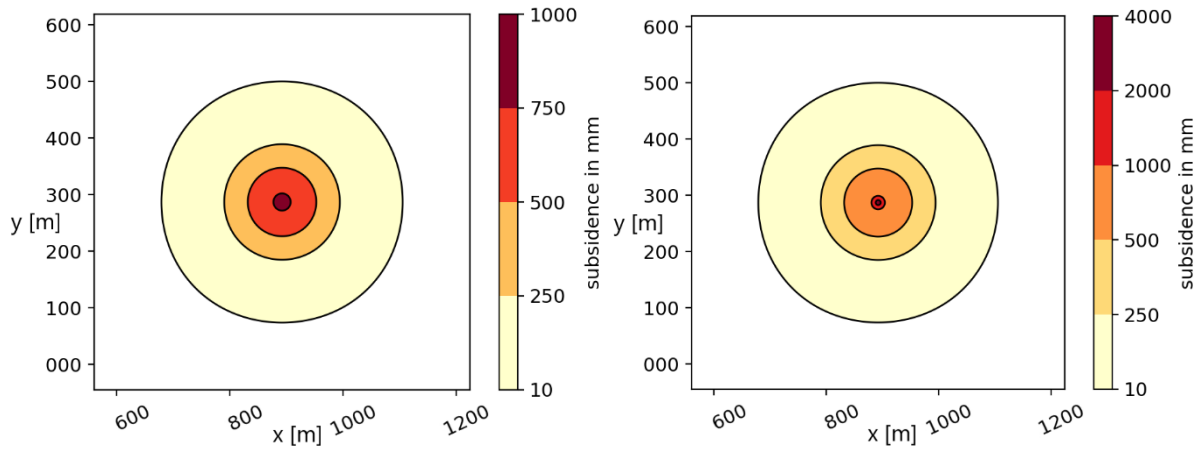

Figure 3. Example of the results from the Bekendam algorithm for phase II (left) and total subsidence (phase II+III, right) in case of a sinkhole with a 2D grid

The Bekendam-Jakob-Pinkse algorithm

The Bekendam-Jakob-Pinkse (BJP) algorithm was developed in 2023 and 2024. It is based on the Bekendam algorithm with some crucial changes. These changes are summarized by the following points.

- Extension from one to three basic cavern shapes
- Reduction of cavern radius during migration (depending on cavern shape)
- New approach for critical depth (depending on cavern radius)
- Five Subsidence stages (instead of three phases)
- Smooth transitions between stages (no subsidence switches between stages)
- Consideration of the influence of backfill behavior

In the BJP algorithm three basic cavern shapes are allowed: cylinder, cone and cylinder + cone. Each shape leads to a corresponding shape of the migration column, which is illustrated in Figure 4.

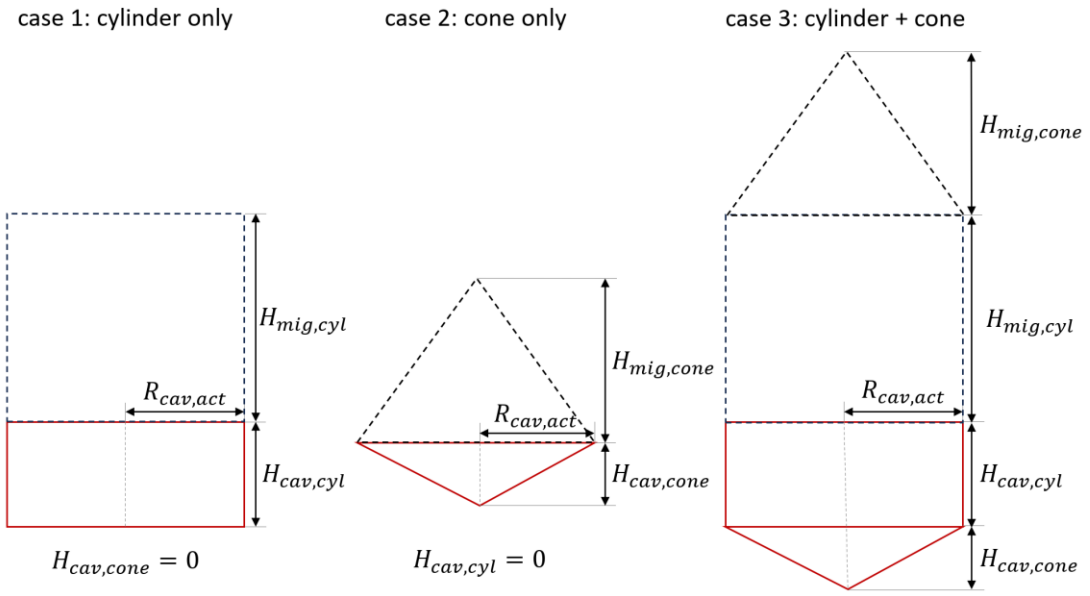

Figure 4. Basic cavern shapes and migration volumes with denotations

In BJP algorithm the migration height of the cylindrical part of the cavern is determined in the same way as in the Bekendam procedure ($H_{mig,cyl} = H_{cav,cyl}/(B-1)$).
In case of cone-shaped caverns the inner angle of the migration cone volume β is derived from geometrical considerations (see Figure 5). The angle β is based on the inability of collapsed rock to (fully) bulk at the outer contour of a cavern with limited height during cavern migration.

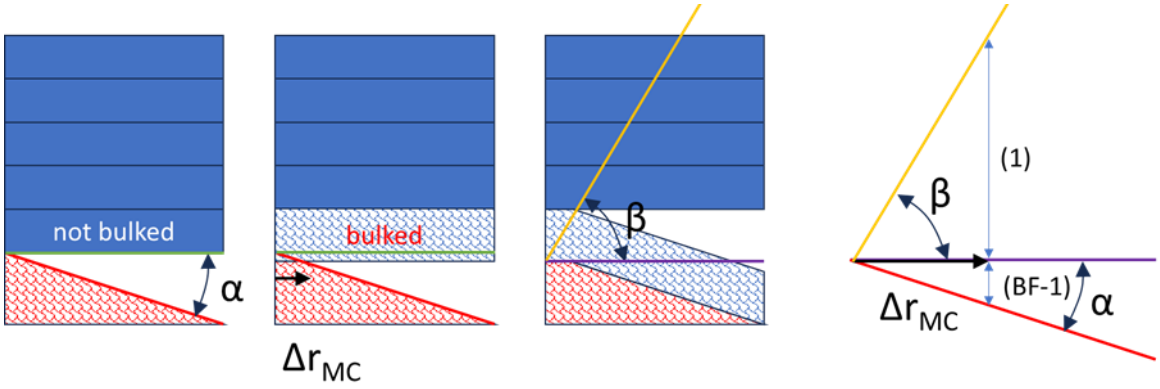

Figure 5. Geometrical solution for radius reduction in the case of cone-shaped caverns

The geometrical solution for calculation of angle β depends on the inner angle α and the bulking factor B.

$$\tan\beta = \frac{H_{mig,cone}}{R_{cav,act}} = \frac{\tan\alpha}{B-1}$$

By insertion of $\tan\alpha = H_{cav,cone}/R_{cav,act}$ into the equation above, the migration height of the conical part can be derived. It is identical to the cylindrical part.

$$H_{mig,cone} = \frac{H_{cav,cone}}{B-1}$$

A new approach for the deflection of the remaining top rock layer, when the cavern migrates near the critical depth was developed. The approach uses the Mohr-Coulomb stress criterion and an empirical equation for bending of a circular plate under equally distributed vertical load. The result is an implicit set of equations, that can be solved iteratively using the critical depth from the Bekendam algorithm as starting value, which is 40 m (131 ft) below depth of the top rock d_{TR}.

$$R_{cav,crit} = R_{cav,act} - \left(d_{Tcav,cyl} - d_{crit}\right) \cdot \tan(90° - \beta)$$

$$d_{crit} = d_{TR} + R_{cav,crit} \cdot \sqrt{\frac{10^{-6} \cdot (\gamma_s - \gamma_w) \cdot d_{crit} \cdot (1 - \sin\varphi)}{10^{-6} \cdot (1 + \sin\varphi) \cdot \gamma_w \cdot d_{crit} + 2 \cdot c \cdot \cos\varphi}}$$

In this solution $R_{cav,crit}$ is the radius of the cavern at critical depth (in the case of conical caverns it is smaller than the radius of the initial cavern and can be determined by the depth of the top of the cavern after migration of the cylindrical part $d_{Tcav,cyl}$ and the inner angle β), γ_s is the unit weight of the sedimentary overburden, γ_w is the unit weight of water and φ and c are the friction angle and the cohesion of the top rock material.

As result of a detailed and comprehensive analysis of subsidence data from numerous migrated and non-migrated caverns, the BJP algorithm distinguishes five possible subsidence stages, see Figure 6.

- Stage 1 subsidence occurs due to creep deformation of the salt. Compared to subsidence of a migrated cavern the amount of stage 1 subsidence is negligible. Stage 1 subsidence corresponds to phase I subsidence (see Bekendam algorithm).

- Stage 2 subsidence occurs, when the cavity migrates upward through the Top Anhydrite and the Claystone above. Stage 2 subsidence corresponds to phase II subsidence (see Bekendam algorithm).

- Stage 3 subsidence is caused by the deflection of the last remaining layer of competent rock over a migrated cavern below the unconsolidated Tertiary soils when the cavern migration reaches the critical depth. Stage 3 subsidence was implemented to enable a more realistic description of the transition from caverns, where the migration process ends near (but below) critical depth and caverns where the migration surpasses the critical depth (transition from stage 2 to stage 4 or Bekendam phase II to phase III, respectively).

- Stage 4 subsidence is caused by the collapse of the last remaining layer over competent rock and subsequent “plug-failure” of the Tertiary soils into the remaining cavern volume. Stage 4 subsidence corresponds to the trough and sinkhole scenarios for phase IIIA subsidence (see Bekendam algorithm).

- Stage 5 subsidence is caused by the consolidation of the bulked overburden under the load of the Tertiary soils. Stage 5 subsidence corresponds to phase IIIB subsidence (see Bekendam algorithm). Stage 5 subsidence replaces stage 3 subsidence.

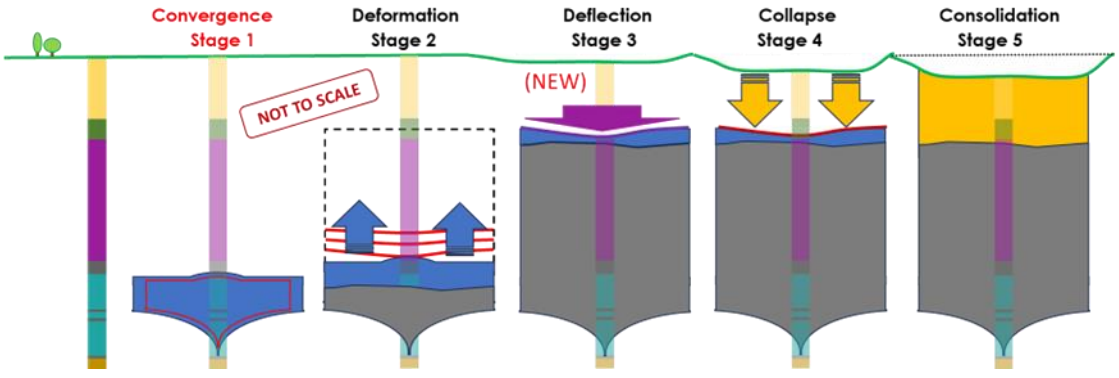

Figure 6. Illustration of subsidence stages for the BJP algorithm

Figure 7 presents a schematic principle for stage 2 to 5 subsidence for a cavern scenario with a case 2 shape (cone only) and a cavern scenario with a case 3 shape (cylinder + cone). In both scenarios the migration ends with the development of trough subsidence.

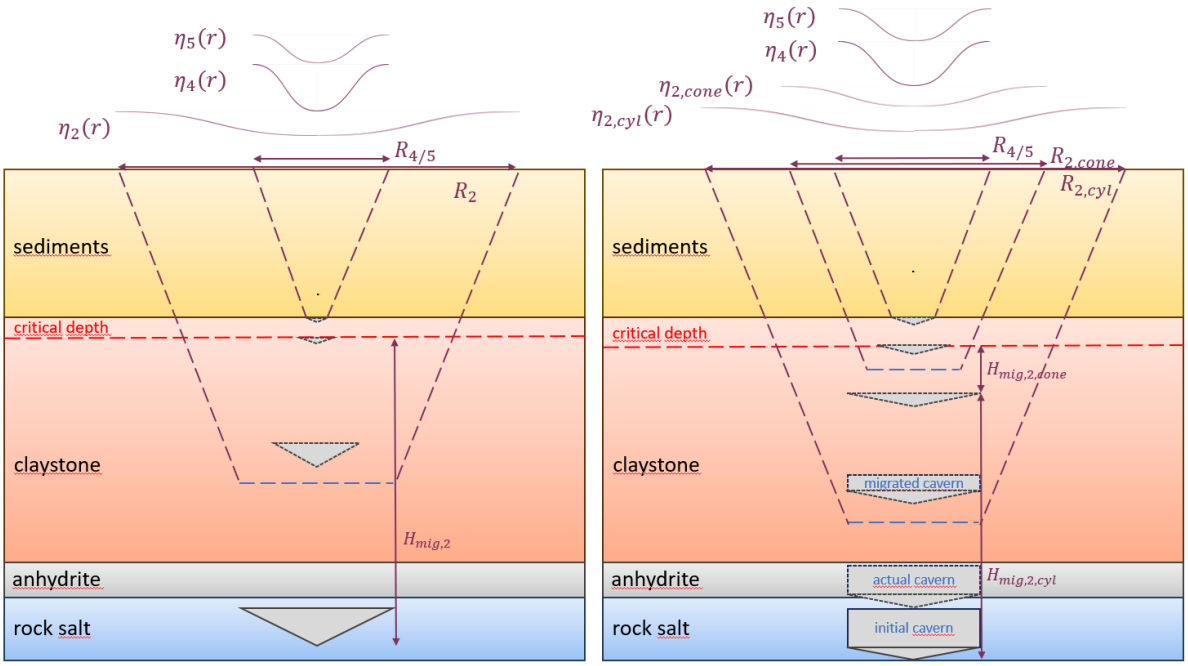

Figure 7. Schematic principle of the subsidence stages for cone (case 2) and cylinder+cone (case 3) cavern shapes using the BJP algorithm.

To consider slurry-backfill for each cavern with the BJP algorithm, two additional input parameters are needed, the volume of unconsolidated backfill solids and a consolidation factor. In the algorithm, the backfill will effectively reduce the height of the cavern. For caverns migrating above the critical depth (stage 4+5) the BJP algorithm outputs the required volume of consolidated backfill to limit the migration to a level below the critical depth (stage 2 only).

The total subsidence from stages 2 to 5 is derived by superposition of all subsidence amounts on a 2D coordinate grid in space (any resolution possible). In addition, the BJP algorithm allows the superposition of subsidence troughs from several adjacent caverns, an example of which is shown in Figure 8.

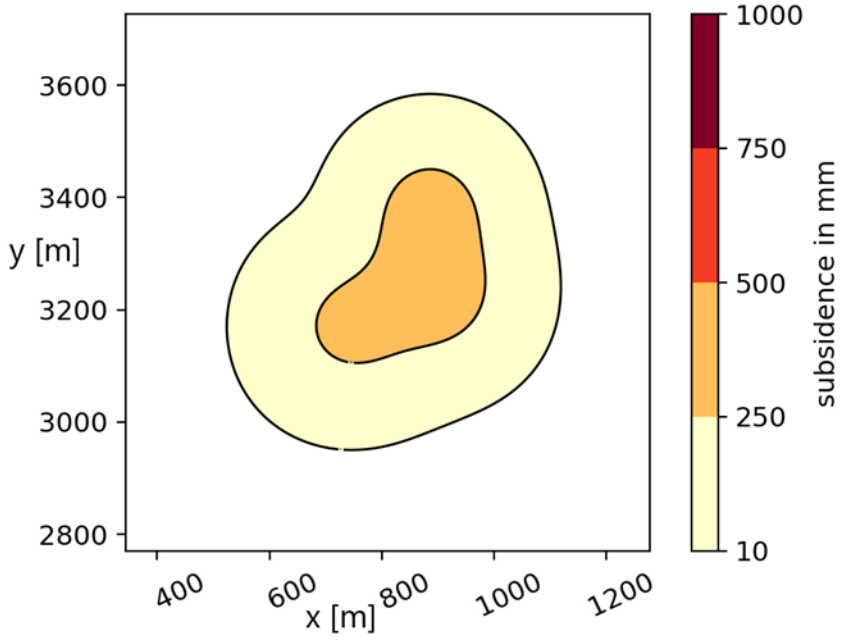

Figure 8. Example of the results from the BJP algorithm with three overlapping subsidence troughs

Validation examples

The validation of the developed BJP Algorithm was achieved by demonstrating that the derived relationships and selected input parameters are applicable to 9 out of 10 well-documented migration cases (REinvent GmbH, 2024). Initial validation of the algorithm was achieved based on the reconstruction of 5 “straightforward” cavern migration cases. The validation was subsequently strengthened by the reconstruction of 4 “complex” migration cases. Furthermore, the applicability of the algorithm to poorly documented migration cases was demonstrated by operating the algorithm in reverse for 2 caverns to reconstruct the migration column and the likely original cavern shape based on the observed subsidence. The validation showed that the algorithm is applicable to the entire TWR area. This validation of applicability focused on the four main input parameters described in the previous paragraph.

1. Effect of cavern shape on migration column shape.
2. Bulking Factor of insolubles, intermediate claystone benches and overburden.
3. Backfill volume balance: actual insitu backfill versus pumped slurry.
4. Backfill behaviour under load: consolidation by self-weight and under load of bulked overburden.

The performed validation process will be illustrated by two examples of cavern migration reconstruction for caverns 15 and 37 taken from Report 3 (REinvent GmbH, 2024). Both caverns have a case 3 shape (cylinder + cone) whereby cavern 15 was backfilled and cavern 37 was not.

Reconstruction cavern 15

Cavern 15 (C15) is a single completion cavern (SCC) developed from well TWR-015 drilled in 1948. After an initial sump phase of approximately three years forming an undercut, the cavern was further developed as a cylinder with a span of nearly 100 m. By 1961, the cavern roof had reached the top of the main salt bed, Salt C, and exposed the overlying claystone bench CD. It can be assumed that this claystone bench quickly collapsed after exposure, consequently exposing the overlying Anhydrite-E to production water. The prolonged exposure of the Anhydrite-E to water led to its deterioration and gradual collapse between 1961 and approximately 1967. This unfavourable situation was acknowledged early on and backfilling of the cavern commenced in 1961 to prevent significant subsidence caused by cavern migration.

The backfill volume used to prevent significant subsidence at cavern 15 is well-recorded and allowed an accurate estimation of the relation between backfill slurry pumped to the cavern and the resulting in-situ unconsolidated backfill in the cavern. Based on historical data an estimated 20% of the slurry consisted of solid material which formed the unconsolidated backfill in the cavern. Assessment of the available sonar images also allowed for an estimation of the self-weight-consolidation (SWC) of the insitu backfill. The SWC was conservatively selected at 15%.

The (partly) backfilled cavern in 1967 is visible in a sonar image from that year, see the magenta shape in Figure 9. The reconstructed cavern is overlain in this figure for comparison. In this figure, the self-weight-consolidated backfill heap is indicated by green, bulked material of the collapsed claystone bench CD indicated by orange and insolubles and intermediate claystone benches fill in the sump indicated by red.

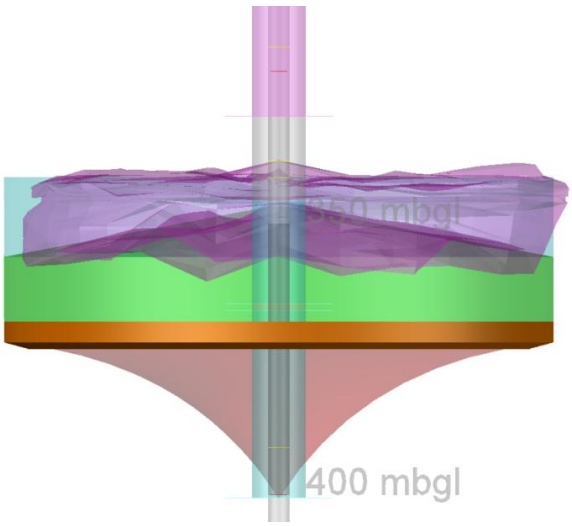

Figure 9. Reconstructed cavern (blue) until 1967 and sonar image (magenta) from 25-09-1967.

The migration history of cavern 15 is very well documented by consecutive sonar measurements, Gamma Ray (GR) logs and observations recorded in the well diary. This allowed for a detailed reconstruction of the migration process following the several sonar images available between 1967 and 1971 as shown in Figure 10. The cavern bottom profile of the sonar images between 1967 (left in Figure 10) and 1971 (right in Figure 10) propagate from a positive (z-direction) cone-shape, via a flat bottom to a negative cone-shape. This visible transition confirms the expected consolidation of the backfill under the load of bulked overburden. Reconstruction of the backfill consolidation volume, as indicated by the orange diamond-shape in Figure 10, was now possible and yielded the consolidation volume of the backfill under the load of bulked overburden.

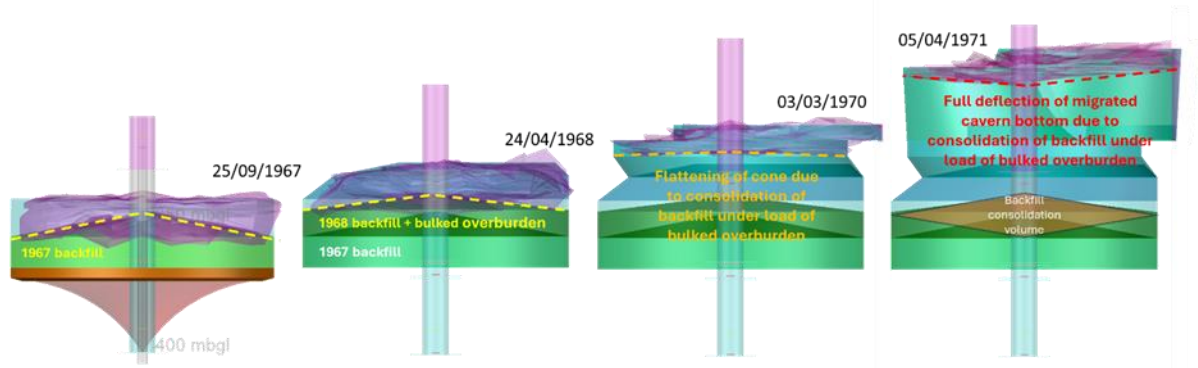

Figure 10. Migration of cavern 15 captured by consecutive sonars between 1967 and 1971. Reconstructed migration column in shades of blue, original sonar images in shades of magenta.

The detailed migration reconstruction of C15 in four steps between 1967 and 1971 allowed for an estimation of the overburden bulking factor. This estimation has also been performed historically for this cavern leading to the used bulking factor value of 1,11. It has been established during the performance of the recent study, that this estimate was made without properly considering the consolidation of the backfill present in this cavern under the load of bulked overburden. In the recent study, the historical estimation was revised to account for this consolidation which led to an estimated bulking factor of approximately 1,2. The effect of accounting for consolidation of backfill during cavern migration is explained by Figure 11.

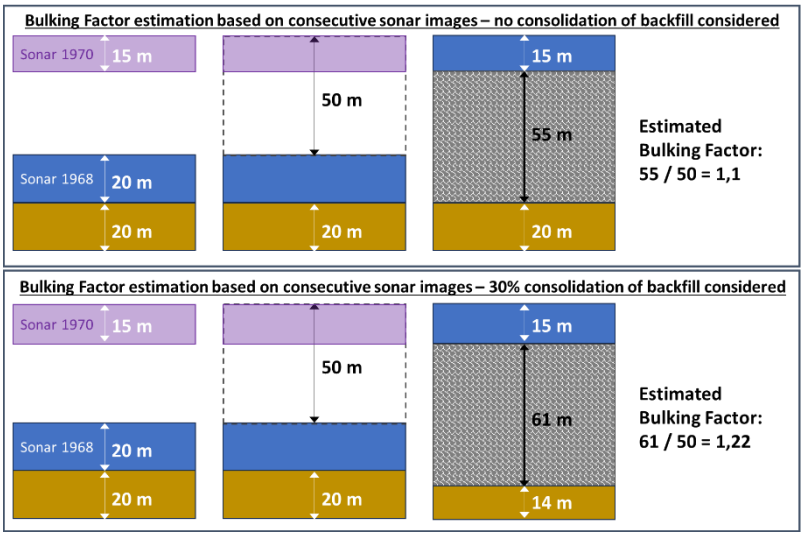

Figure 11. Cavern 15: Estimation of the bulking factor from consecutive sonar images during migration. Top picture – not considering backfill consolidation; Bottom picture: considering 30% consolidation

In the top picture of this figure, a model representation of the sonar images from 1968 and 1970 at cavern 15 is shown in the left picture. The 1968 sonar in blue with the backfilled portion of the cavern in brown. The consecutive sonar capturing the migration process from 1970 is shown in lilac. The distance between the cavern roofs of the consecutive sonar is shown in the middle picture. Please note

that the shown dimensions are not necessarily reflecting the actual situation at cavern 15, rather are chosen to ease this exemplary estimation.

When the bulking factor is estimated from the just described model representation, i.e. without considering consolidation of the backfill in the cavern, the situation in the right picture is leading, i.e. the backfill height remains 20 m as shown. The bulking factor is therefore estimated at:

BF = Bulked overburden height (55 m) / Intact overburden height (50 m) = 1,1

In the bottom box of Figure 11, the same model representation of the sonar images from 1968 and 1970 is shown, however now considering consolidation of the backfill in the cavern. The original backfill height of 20 m is thus reduced by 30% to 14 m due to the load of the bulked overburden. As can be seen, the estimated bulking factor is now higher and is estimated at:

BF = Bulked overburden height (61 m) / Intact overburden height (50 m) = 1,22

This principle is a fundamental difference between the Bekendam method and the BJP approach and significantly influences the way migration is calculated. Consequently, this principle also influences the amount of subsidence that can develop due to cavern migration.

When accounting for consolidation of the backfill in cavern 15 between 1967 and 1971, an average bulking factor of 1,20 is found to best suit the volume reconstruction. This fitment is based on the inclusion of 30% additional consolidation of the backfill under the load of the bulked overburden, i.e. in addition to the 15% SWC. The value of 1,20 is thus applied for this cavern and has further validated by the reconstruction of other well-documented cavern migration cases during the study.

Sonar images that could document the further migration of cavern 15 after 1971 are not available. However, several other observations, mainly gamma ray logs and notes on obstructions in the well diary, did enable a qualitative initial reconstruction of the migration column after 1971. This reconstruction also allowed for a direct comparison with the Bekendam method. The observations from sonar images and notes from the well diary are graphically organized in Figure 12.

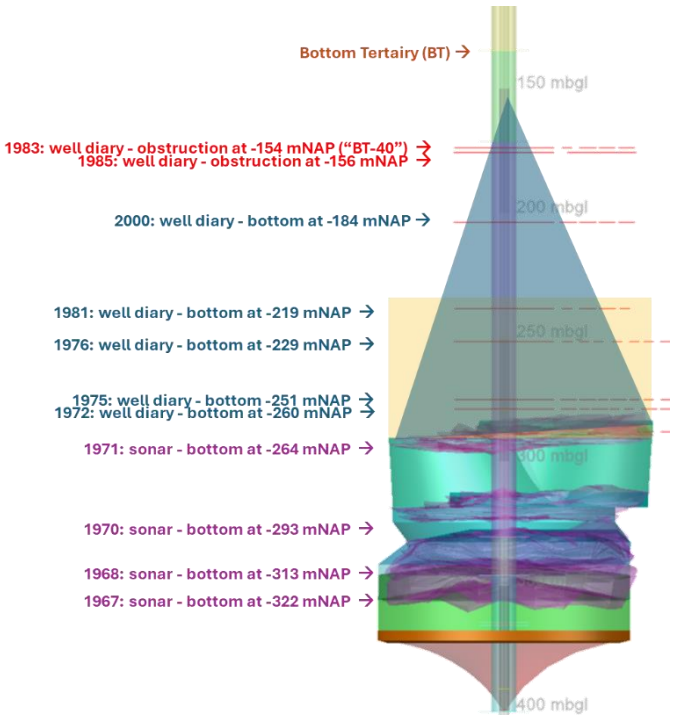

Figure 12. Migration column development at cavern 15 between 1967 and 2000. The decreasing depth of the cavern bottom is indicated based on sonar (purple), well diary notes (blue) and obstruction observations due to most likely pulled-apart casing pipes (red). The favoured migration column development after 1971, with a reducing column diameter (cone-shaped) is indicated by the blue triangle. The alternative cylindrical migration column after 1971 is indicated by the yellow rectangle.

The recorded observations in the well diary allow for two possible overall migration scenarios:

1. A cylindrical migration column after 1971 using a bulking factor of approximately 1,2 thus reaching a depth of approximately 240 mbgl (787 ftbgl), shown as the light-yellow cylinder in Figure 12.

2. A cone-shaped migration column after 1971, using a bulking factor of approximately 1,2 reaching a depth of approximately 150 mbgl (492 ftbgl), shown as the dark blue cone in Figure 12.

The cone-shaped migration fits best with the well diary notes recorded between 1971 and 2000 as the cylinder does not reach the depth of the residual cavern recorded in 2000. The cone shaped migration on the other hand exceeds the depth of the recorded bottom in 2000 at approximately 204 mbgl (669 ftbgl). This is in line with the expected transition between collapsed, bulked overburden in the "mobilized zone" and delaminated overburden, which has not collapsed just deflected, in the "yielded zone". An "air gap" separates these two zones. A detailed explanation of the several zones in a migration column is provided in Figure 13.

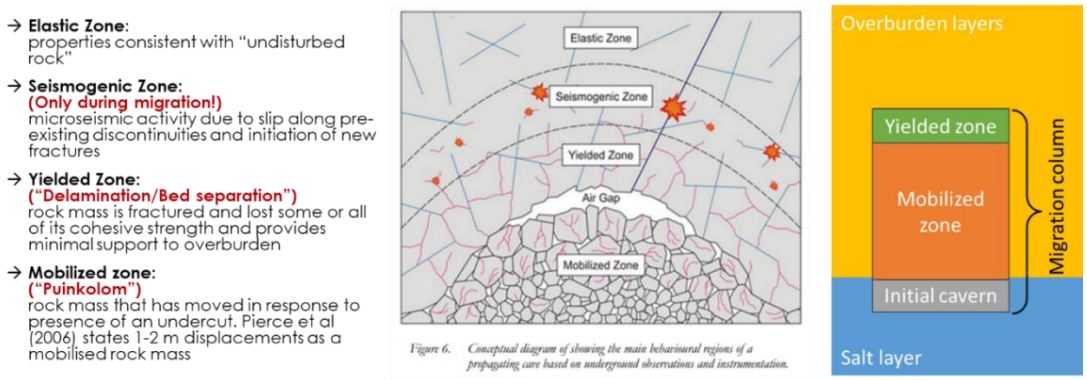

Figure 13. Subdivision of migration column in zones: (from top to bottom) elastic, seismogenic, yielded and mobilized (adapted from (Sainsbury, 2012)).

The just described qualitative migration history of cavern 15 using a cone-shaped migration column after 1971, rather than the continuation of the prior cylindrical migration was validated using the BJP -Algorithm. This validation is partly based on the depth of the transition between the mobilized and yielded zones as confirmed by the available gamma ray logs.

Reconstructio of migration and subsidence of cavern 15

The application of the BJP Algorithm to the reconstructed migration of cavern has been performed using a subsidence prognosis work process developed during the study. The potential migration column radius is a critical input parameter. This radius was determined by converting the surface area of the maximum cavern contour into circle. The determination of this area was achieved by construction of an intersection plane between the cavern volume, as represented by the 1967 sonar image, and the Top of Salt C, as per the stratigraphy description for this cavern. The construction of this intersection is shown in Figure 14, left image, and indicated by the red contour.

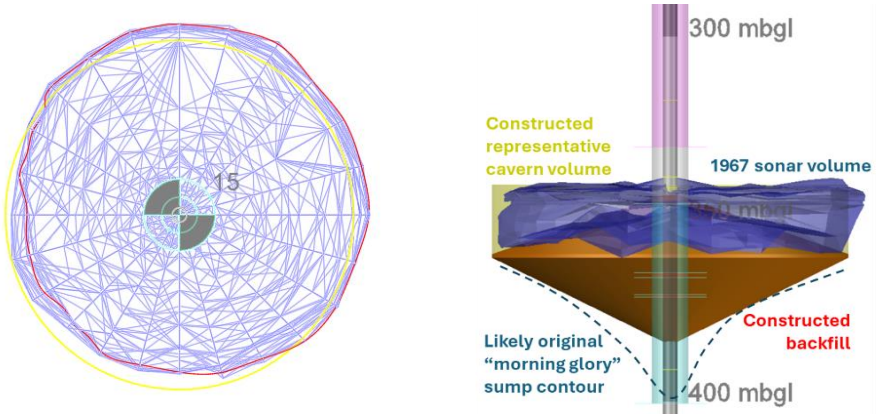

Figure 14. Left image: Intersection of Top Salt C with cavern 15 volume based on the 1967 sonar image in blue, actual intersection in red, simplified cavern contour in yellow. Right image: reconstruction of „Representative volume" (yellow) and constructed backfill volume in 1967 (brown).

The volume of the representative cavern volume is based on the salt production and the cavern reconstruction. A set of input parameters for the BJP Algorithm was derived based on the reconstruction of all relevant geometries as shown in Figure 14. Using the selected input parameters, the BJP Algorithm produced the output presented in Figure 15. This figure compares the available sonar images (left picture) with a graphical representation of the algorithm output (right picture).

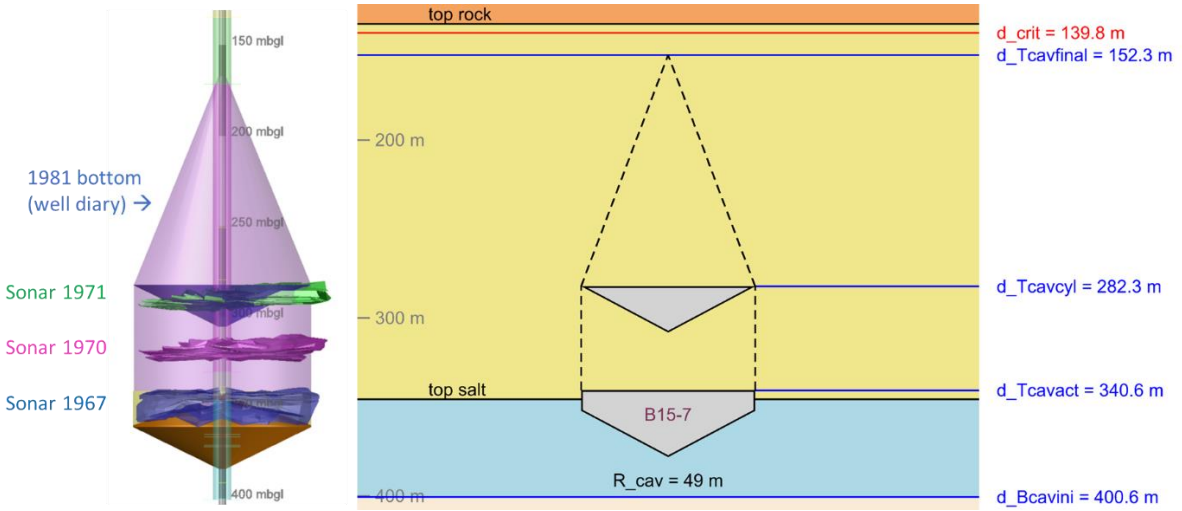

Figure 15. Left image: Comparison of the observed migration of cavern 15 from sonar images, right image: calculated output of the BJP Algorithm.

As can be seen from Figure 15, the BJP Algorithm has determined that the migration process of cavern 15 includes both a cylindrical and a conical part based on the cavern geometry. The migration of cavern 15, accounting for the backfill, reaches 152,3 mbgl (500 ftbgl), staying well away from the critical depth of 139,8 mbgl (459 ftbgl).

The conical top of the migration column contains the transition between the bulked overburden (the mobilized zone) and deflected overburden strata (yielded zone) near the top of the migration cone. The actual position of this transition (air gap) is most likely around 200 mbgl (656 ftbgl), where the cavern bottom was observed in 2000, see Figure 13. The deflection of the strata above the final cavern bottom can be observed from the available Gamma Ray logs (GR-logs) as is shown in Figure 16.

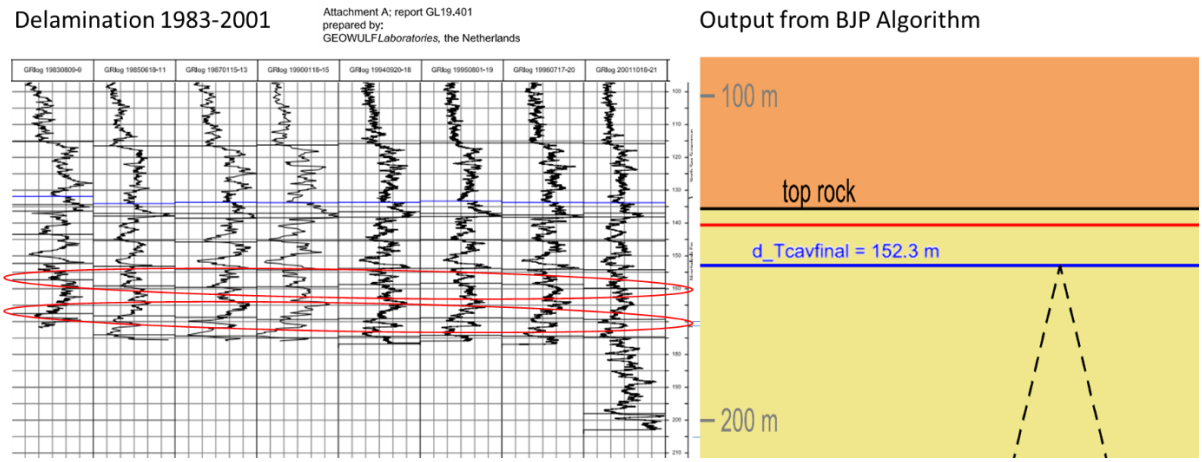

Figure 16: Cavern 15 migration: deflection of strata near top of the migration column as observed from GR logs 1983-2001 (adapted from Attachment A to (GEOWULF Laboratories, 2019)).

The blue marker near the top rock in the left image does not move at all between 1983 and 2001, whilst the markers within the red ellipses show a slight but gradual deflection over this same time period. This gradual deflection represents the formation of the yielded zone above the mobilized zone as the migration approached its final depth. The estimated and consequently used bulking factor of 1,20 thus includes both the mobilized zone and the yielded zone in addition to any air gap that is left behind after the migration of a cavern is completed. As such a bulking factor of 1,20 can be considered an average value for the migration column, not a maximum value.

As a result of migration of cavern 15, only Stage 2 (and a negligible amount of Stage 3 subsidence) is developed, in line with the observed subsidence. Stage 4 (trough/sinkhole) formation and subsequent Stage 5 subsidence do not occur, again in line with the observed subsidence. The output of the BJP Algorithm also comprises graphical representations of the subsidence contours and all its derivatives. The calculated subsidence contour for cavern 15 is shown in Figure 17. The measured subsidence is also shown in this figure for comparison.

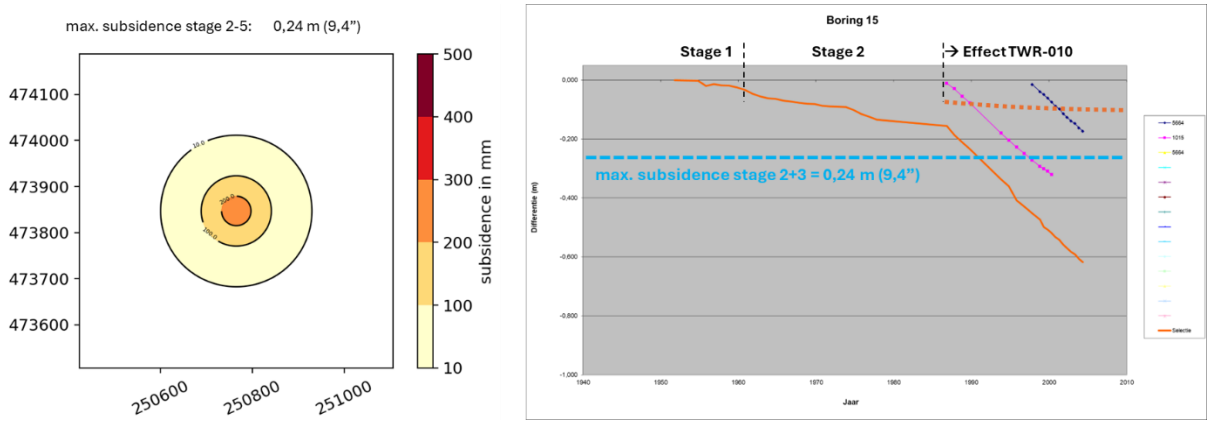

Figure 17: Cavern 15: subsidence contours as calculated by the BJP Algorithm (left image) and actual measured subsidence (right image).

As can be seen from this figure, the calculated subsidence fits well to the actual measured subsidence considering the influence of the subsidence bowl caused by migration at well TWR-010 after 1986. It must be noted that the calculated subsidence is independent of time as it is simply the total subsidence calculated by the algorithm base on the input parameters. The actual subsidence will slow down over time as the migration approaches its final depth thus not showing the maximum value in the measured subsidence. In conclusion, the application of the BJP Algorithm to the cavern migration and subsequent subsidence development for cavern 15 shows the applicability of the chosen methods and parameters and thus supports the validation process.

Reconstruction of migration and subsidence of cavern 37

The validation of the algorithm is further illustrated by the reconstruction of cavern development, migration and subsequent subsidence development of cavern 37. This cavern is similar to cavern 15 in terms of shape, but no backfill has been applied thus simplifying the reconstruction process and demonstrating that the selected bulking factor of 1,20 is also valid for caverns without backfill. As the description of the reconstruction processes for C15 has been elaborate, the level of detail in this description is limited to streamline this paper.

Cavern 37 is a single completion cavern from well TWR-037 drilled in 1955. After an initial sump phase of approximately three years forming an undercut, the cavern was further developed by extending and widening this contour upwards for the years 1958 and 1959. After 1959, the cavern developed cylindrically upwards until it reached the top of the main salt bed, Salt C. The final shape of the reconstructed cavern is shown in Figure 18 and volume of the final reconstructed cavern is 75.010 m³.

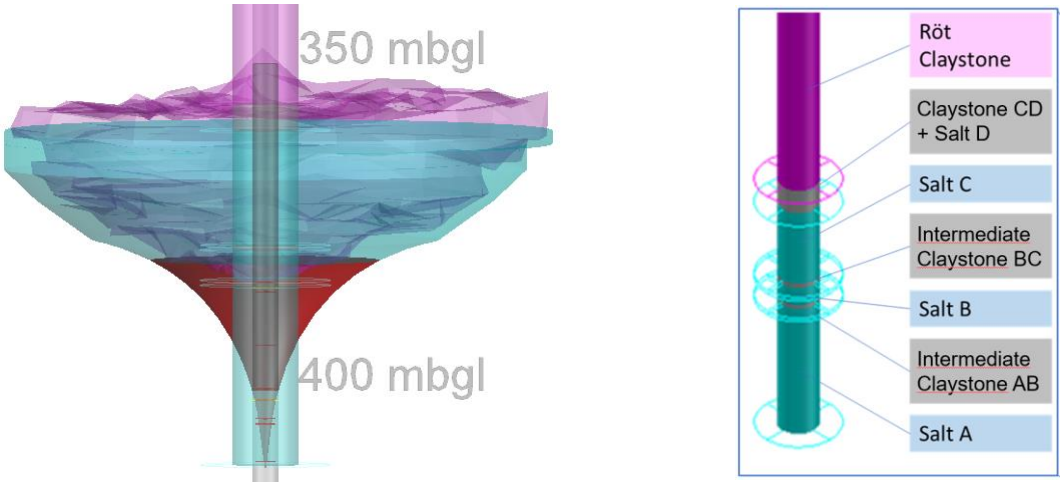

Figure 18: Cavern 37: final reconstructed cavern (blue) until 1967 and sonar image (magenta) from 1971. Claystone bench and insolubles fill visible in red.

The sonar image of 1971 shows that the actual cavern has extended vertically into the overburden layers after 1967. This position could be caused by either gradual disintegration or sudden collapse of the claystone bench CD layer. The higher cavern bottom in the sonar image compared to the reconstruction, indicates that this could be the bulked claystone bench CD.

To accommodate for the collapse of the claystone bench CD in the reconstruction, the cavern volume as shown in Figure 18 was updated with this event. A visual representation of the roof collapse of claystone bench CD is shown in Figure 19. The collapsed claystone bench CD at the top of the cavern is indicated by light grey, whilst the bulked material on the bottom of the cavern is indicated by orange. The volume of the 1971 sonar image is 71.800 m³ which is a near perfect correlation to the reconstructed volume in 1971 (71.676 m³).

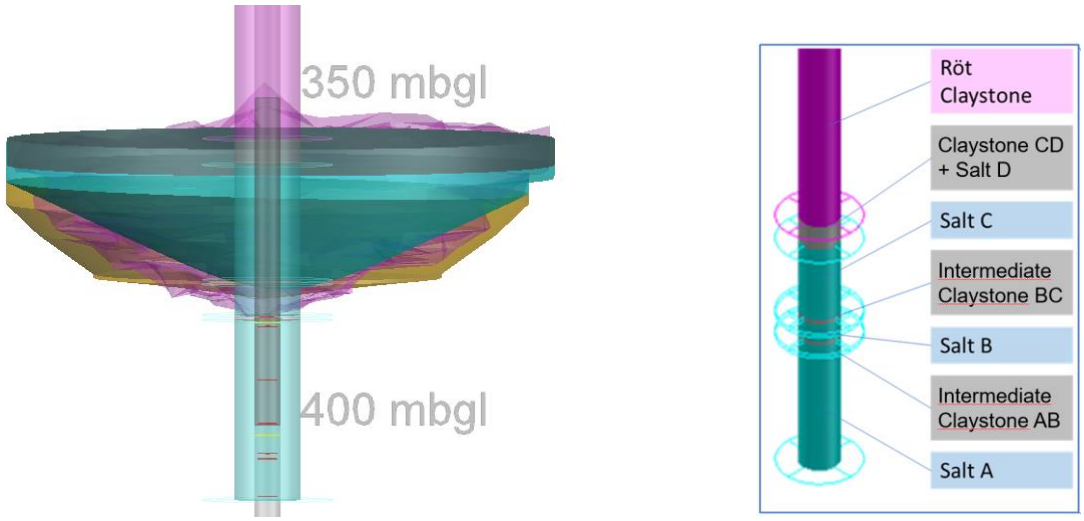

Figure 19: Reconstructed cavern (blue) until 1971 and sonar image (magenta) from 1971. Collapsed claystone bench CD indicated by grey and its bulked overburden as orange.

The presence of Anhydrite-E is not noted on the drilling log and gamma ray logs for this depth interval are not available. Nonetheless, it is likely that Anhydrite-E was present at this cavern since nearby wells do show its presence. Notwithstanding a (semi-)competent Anhydrite-E layer above the collapsed claystone bench CD in 1971, migration is observed for this cavern after 1967 according to well diary recordings (“bend pipes”) and gamma ray logs from later years.

The migration of cavern 37 was reconstructed manually using 3D CAD software and using the BJP Algorithm. The output of the manual and algorithm reconstructions have been compared to the available observations from gamma ray logs in Figure 20.

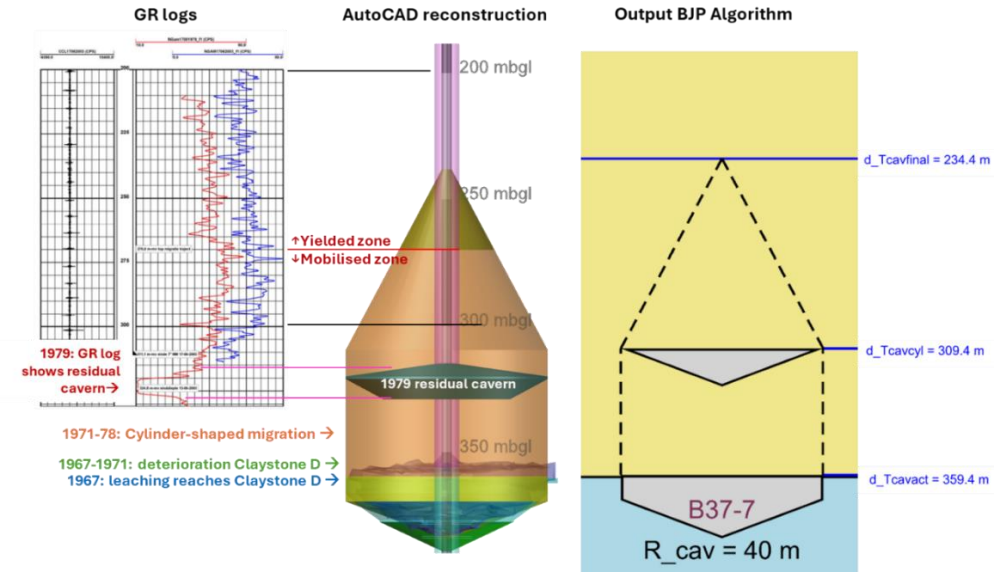

Figure 20: Cavern 37: Comparison BJP Algorithm output and observations from GR logs

The calculated subsidence contours for cavern 37 are shown in Figure 21. The actual measured subsidence at cavern 37 is also shown in this figure for comparison.

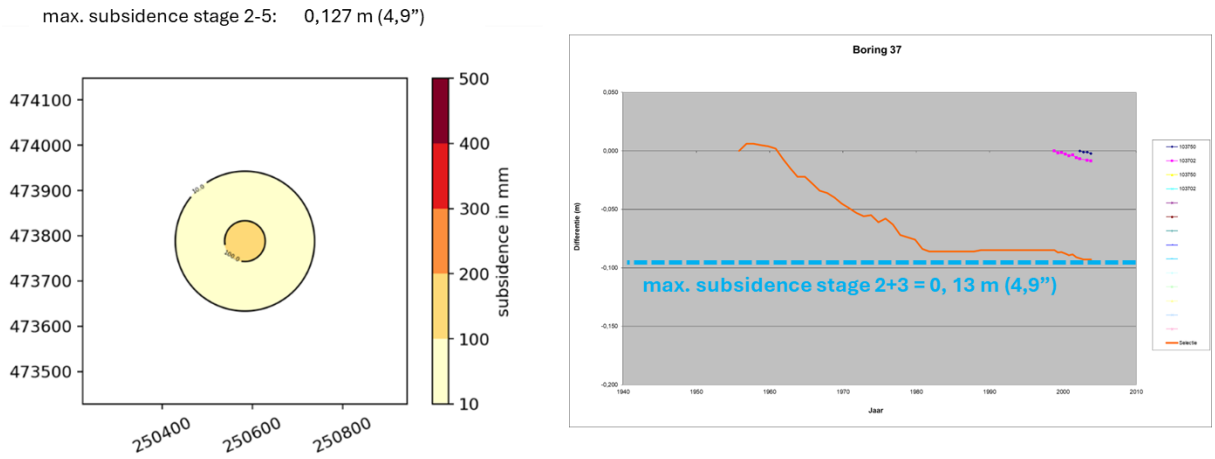

Figure 21: Cavern 37: subsidence contours as calculated by the BJP Algorithm (left image) and actual measured subsidence (right image).

As can be seen from this figure, the calculated subsidence fits well to the actual measured subsidence. In conclusion, the application of the BJP Algorithm to the cavern migration and subsequent subsidence development for cavern 37 shows the applicability of the chosen methods and parameters for a cavern without backfill and thus supports the validation process.

Conclusion

The validation of the BJP Algorithm has been achieved by demonstrating that the derived relationships and selected input parameters are applicable to the well-documented cavern migration cases. Initial validation of the algorithm was achieved based on the reconstruction of 5 cavern migration cases. The validation was strengthened by the reconstruction of 4 additional complex migration cases. The applicability to poorly documented migration cases was demonstrated by operating the algorithm in reverse for 2 caverns to reconstruct the migration column and the likely original cavern shape based on the measured subsidence and salt production figures.

The validation shows that the BJP Algorithm is applicable to the entire TWR area. The validated applicability focused on the four main input parameters:

1. Effect of cavern shape on migration column shape.
2. Bulking Factor of insolubles, intermediate claystone benches and overburden.

3. Backfill volume balance: actual insitu backfill versus pumped slurry.
4. Backfill behaviour under load: consolidation by self-weight and under load of bulked overburden, as well as lack of bearing capacity of top layer of backfill (thickness is assumed to be 2 m or 6,6 ft).

At each stage of the parameter selection process care was taken to maintain a conservative but realistic approach. The main conservatisms used in the reconstruction and the parameter selection process are:

- Introduction of the radius reduction mechanism based on a cone-shaped cavern (bottom) leading to higher migration column potential compared to purely cylindrical migration columns as historically used.
- Analysis of actual cavern shape, volume and position in the stratigraphy as the basis for a representative cavern volume compared to the use of only cavern height as a measure for migration potential as historically applied.
- Determination of representative cavern volume on salt production rather than sonar volume, consequently considering sonar shadow and other sources of volume underestimation resulting from sonar inaccuracy.
- Use of a Bulking Factor of 1,2 as opposed to the historically used Bulking Factor of 1,11. Considering the currently used volume approach for calculating the Bulking Factor, the value of 1,2 is still deemed conservative based on the results of the validation process.
- Backfill application based on the actual pumped slurry volume and with self-weight consolidation, consolidation under load of bulked overburden and a lack of bearing capacity in the top layers considered in the volume balancing. Historically, backfill height was simply subtracted from cavern height to estimate the resulting migration column height, thus not accounting for realistic backfill behaviour.

The result of this approach is an updated and validated prognosis method for potential subsidence caused by cavern migration in the TWR area, i.e. the BJP Algorithm. The methodology and the results should be continuously updated when new information arises from the operation of caverns in the Hengelo brinefield.

Acknowledgements
The authors would like to thank Nobian Industrial Chemicals B.V. for their cooperation and team spirit during the performance of this study. The tireless attention to detail demonstrated by the members of the MDC team have elevated the overall quality of the work performed and reports delivered.

References

R. F. Bekendam, „ Stoping in Weak Rock over Salt Solution Cavities in the Hengelo Field, The Netherlands, and Its Expression in Terms of Surface Subsidence (meeting paper),“ Solution Mining Research Institute, Cracow, Poland, 1997.

GeoControl, „Bepaling van de mogelijke toekomstige bodemdaling ter plaatse van de Rijksweg A35, Versie 2, Rapport S00607,“ 2006.

GEOWULF Laboratories, “Geological Framework TWR Area Compilation Report Volume I (GL08.502)”, 2008

GEOWULF Laboratories, “TWR North identification of delamination based on GR logs,” 2019.

REinvent GmbH, “Report 3 - Validation of the input parameters by the assessment of migration behavior of migrated caverns and determination of the likelihood of migration.”, Sondershausen, 2024

B.-A. L. Sainsbury, “A MODEL FOR CAVE PROPAGATION AND SUBSIDENCE ASSESSMENT IN JOINTED ROCK MASSES,” The University of New South Wales, Sydney, 2012.